Hindawi
Geofluids
Volume 2023, Article ID 3072665, 9 pages
https://doi.org/10.1155/2023/3072665

Research Article

Research and Application of Optimization Technology for High-Efficiency Fracturing and Packing Parameters of Unconsolidated Sandstone

Liwei Sun

Engineering and Technology Research Institute, CNPC Great Wall Drilling Engineering Company Limited, Panjin 124010, China

Correspondence should be addressed to Liwei Sun; lh_sunlw@163.com

Received 22 August 2022; Revised 22 September 2022; Accepted 26 September 2022; Published 22 March 2023

Academic Editor: Dan Ma

The fracturing and filling technology is expected to meet the dual needs of production stimulation and sand control of unconsolidated sandstone reservoirs, but there is no clear guiding method for the optimization of construction parameters, which hinders its efficient development. In order to study the optimization technology of high-efficiency fracturing and packing parameters in loose sandstone, this paper takes a loose sandstone reservoir in Liaohe Oilfield as the research object and firstly studies the fracture initiation and extension laws of loose sandstone fracturing based on really well and formation data and takes this as a physical. The model explores the migration law of proppant under different working conditions. Research shows that (a) the layered fracturing is more likely to form a fracture shape that meets the dual needs of filling and production enhancement. (b) Increasing the viscosity of the sand-carrying fluid is conducive to the migration of proppant to the far end, and increasing the sand ratio will make the proppant more easily suspended in the fracture, but it is not conducive to remote migration. (c) Taking "increasing viscosity + increasing sand ratio in a small range" as the optimization idea, the ideal filling parameters are preferably 85 mPa•s sand – carrying fluid viscosity + 15%sand ratio. The field application results show that the daily oil production of three wells after adopting this optimization method is 2.5-3.4 times higher than that of the adjacent wells at the initial stage of production and after stable production.

1. Preface

China's loose sandstone oil and gas resources are widely distributed and shallowly buried, and its efficient exploration and development is of great significance to the realization of stable and increased production of China's oil and gas resources [1]. The fracturing and filling technology has two functions of stimulation and sand control and is the main means to improve the development effect of loose sandstone [2]. Reasonable determination of operating parameters and establishment of on-site construction optimization methods are the keys to efficient development.

Scholars at home and abroad pay more attention to the fracture propagation mechanism and control methods of hydraulic fracturing in tight reservoirs, and there are relatively few researches and understandings on the fracturing and packing technology of loose sandstone. In terms of the basic characteristics of loose sandstone, it is generally believed that the burial is shallow, and the compaction effect is weak [3, 4]. Lao obtained the physical parameters of the loose sandstone and its nonlinear seepage through microscopic pore network simulation [5]. In terms of the physical and mechanical mechanisms of fracture formation in loose sandstone, Deng et al. studied the influence mechanism of geological factors and engineering measures on the initiation and extension of fractures in loose sandstone [6]. According to Agarwal and Sharma, the influence of fracture initiation and extension, it is considered that tensile shear failure is the main mode [7]. Zhao et al. considered the infiltration effect of fracturing fluid and analyzed the fracture mode based on the elastic zone and plastic zone of the unconsolidated sandstone formation [8]. Lin et al. found that a lower elastic modulus is likely to cause short and wide fractures and advocated the use of high injection rate and high

viscosity fracturing fluid [9]. Zhang et al. believed that high sand ratio, low displacement, and continuous slug sanding technology should be used to achieve end screenout [10]. Fan et al. believed that high efficiency fracturing fluid induced fractures short and wide, and it can achieve the purpose of filling and sand control [11]. Li et al. studied the critical sand production rate and sand production area of unconsolidated sandstone fracturing packing based on the fluid-solid coupling model [12].

Based on the above studies, it can be seen that most of the fracturing and filling technologies of loose sandstones remain in qualitative research, and there is still a lack of optimization methods for filling parameters to achieve efficient development. Based on the actual drilling and formation data in the study area [13, 14], this paper studies the fracture initiation and extension mechanism of unconsolidated sandstone fracturing through numerical simulation and uses this as a physical model to further explore the migration law of proppant between them under different working conditions and then optimization to get the most reasonable filling parameters.

2. Fracture Initiation and Propagation Mechanism in Unconsolidated Sandstone

2.1. Fracture Propagation of Unconsolidated Sandstone Hydraulic Fracturing. Unconsolidated sandstone has the characteristics of weak cementation, low strength, strong plasticity, high porosity, and permeability, which makes its fracturing fluid filtration, formation failure characteristics, and permeability evolution law in the fracturing process obviously different from those of conventional rocks. The main manifestations are the change of effective stress in the near-wellbore area caused by the filtration of fracturing fluid, the significant effect of wellbore-formation solid-liquid two-phase coupled flow, and the short and wide fracturing fractures formed, which often require filling to achieve effective sand control.

The commonly used linear elastic fracture mechanics theory considers the difficulty of solving the numerical calculation caused by the stress singularity at the crack tip. The model mainly includes

(1) TS constitutive relation governing the mechanical behavior of cracks [15]

The quadratic nominal stress rule and the linear damage evolution rule are used to judge the fracture initiation behavior of unconsolidated sandstone during fracturing, as shown in the following equation:

$$\left(\frac{\langle t_n\rangle}{t_n^0}\right)^2+\left(\frac{\langle t_{s1}\rangle}{t_{s1}^0}\right)^2+\left(\frac{\langle t_{s2}\rangle}{t_{s2}^0}\right)^2=1, \tag{1}$$

where t_n^0, t_{s1}^0, and t_{s2}^0 are the cohesive normal stress, respectively, the nominal stress of the first shear stress and the second shear, Pa; t_n, t_{s1}, and t_{s2} are the corresponding ultimate nominal stress, Pa; $\langle\ \rangle$ are Macaulay brackets, representing that the compressive stress will not cause damage, as shown in the following formula.

$$\langle t_n\rangle=\begin{cases} t_n, & t_n\geq 0,\\ 0, & t_n<0. \end{cases} \tag{2}$$

When the cohesive stress satisfies the condition of formula (1), the unit begins to be damaged, and the needle crack starts to crack. The cohesive stress will gradually decrease with the opening of the crack, and when it decreases to 0, it indicates complete damage.

(2) Tangential flow inside the opened fracture [16]

Poiseuille's law is used to describe the fluid flow behavior in fractures:

$$q=-\frac{w^3}{12\mu}\nabla p. \tag{3}$$

At the same time, the fluid mass conservation equation can be expressed as

$$\frac{\partial w}{\partial t}+\nabla\cdot q+(q_t+q_b)=Q(t)\delta(x,y), \tag{4}$$

where q is the tangential fluid velocity in the fracture, m^2/s; p is the fluid pressure in the fracture, Pa; q_t and q_b are the normal flow velocity of the upper and lower surfaces of the fracturing fluid cohesion unit, m/s; w is the fracture width, m; μ is the injected fluid viscosity, Pa s; $\delta(x,y)=1$ represents the injection point, and $\delta(x,y)=0$ represents the fracture tip.

(3) The normal flow of fluid in fractures into the reservoir [17]

The normal flow velocity in equation (4) is obtained by the traditional Carter filter loss model:

$$\begin{cases} q_t=\dfrac{2C_{wt}}{\sqrt{t-\tau(x)}},\\ q_b=\dfrac{2C_{wb}}{\sqrt{t-\tau(x)}}. \end{cases} \tag{5}$$

In the formula, C_{wt} and C_{wb} are the filter loss coefficient of the upper and lower surfaces, respectively, m/(Pa•s); t is the injection time, s; $\tau(x)$ is the characteristic time at the position x.

According to the above control equation and the numerical simulation process, this paper firstly couples the physical properties and stress of the reservoir and uses the secondary development subroutine to carry out complex processes such as implicit shear fracture propagation and explicit tensile fracture propagation.

2.2. Fracture Propagation Law of Unconsolidated Sandstone Hydraulic Fracturing. Based on the actual data of Well Huan 1 in the study area, the propagation law of loose sandstone under general fracturing and layered fracturing was studied. First, a physical model was established based on the data in Table 1.

Table 1: Field data of Well Huan 127-25-351.

Horizon	Layer number	Interpret the oil reservoir in the well interval		Thickness (m)	Porosity (%)	Penetration (10^{-3} μm^{2})	Watery saturation (%)	Muddy content (%)	Explain result
		Top bound	Bottom bound						
Xing II	25	816	824	8.0	35.5	4235.2	26.8	1.1	Heavy oil layer
Xing II	28	831	834.9	3.9	33.2	3659.3	44.5	1.4	Heavy oil layer
Xing II	30	842	844.8	2.8	33.9	3577.3	36	1.3	Heavy oil layer

Table 2: Simulation data of each sublayer.

Parameter	Floor number 25		Floor number 28		Floor number 30	
	Reservoir	Compartment	Reservoir	Compartment	Reservoir	Compartment
Elastic modulus (GPa)	5	8	5.2	8.2	5.5	5.5
Poisson's ratio	0.27	0.32	0.28	0.32	0.3	0.35
Permeability (mD)	2854.6	3 054.6	2444.6	2644.6	1 822.2	2 022.2
Horizontal minimum principal stress (MPa)	12.2	12.2	12.4	12.3	12.6	12.5
Horizontal maximum principal stress (MPa)	17.3	17.2	14.1	14.1	17.5	17.4
Overlying pressure (MPa)	22.1	20	22.3	22.2	22.5	22.4
Void ratio	0.355	0.355	0.332	0.332	0.339	0.339
Rock tensile strength (MPa)	0.2	0.2	0.24	0.24	0.26	0.26
Fracture energy (J/m $^{2)}$	100	300	105	315	100	300
Filter loss coefficient (m/$\sqrt{s}$)	8e-12	8e-13	8e-12	8e-13	8e-12	8e-13
Fracturing fluid viscosity (cp)	50	50	50	50	50	50

Build three continuous "interlayer -reservoir-interlayer" models. In the mesh module, the three-layer reservoir to be fracturing is meshed, and the entire model is meshed; after the division is completed, according to Table 2, physical parameters of each layer are displayed, and the established model is shown in Figure 1, and the fracture extension of general fracturing and layered fracturing is shown in Figure 2.

It can be seen from Figure 2 that, in general, the total cross-sectional area of fractures formed by layered fracturing is much larger than that of general fracturing. Therefore, in hydraulic fracturing of loose sandstone, layered fracturing is preferred. When fracturing in different layers, the formation permeability is a key factor affecting the filtration of fracturing fluid and thus controlling the fracture extension shape. From the fracture extension shape of each layer in Figure 2(b), it can be seen that with the increase of reservoir permeability, the smaller the fracture length, the larger the fracture width and height, this is because when the formation permeability is low, the fracturing fluid filtration is limited.

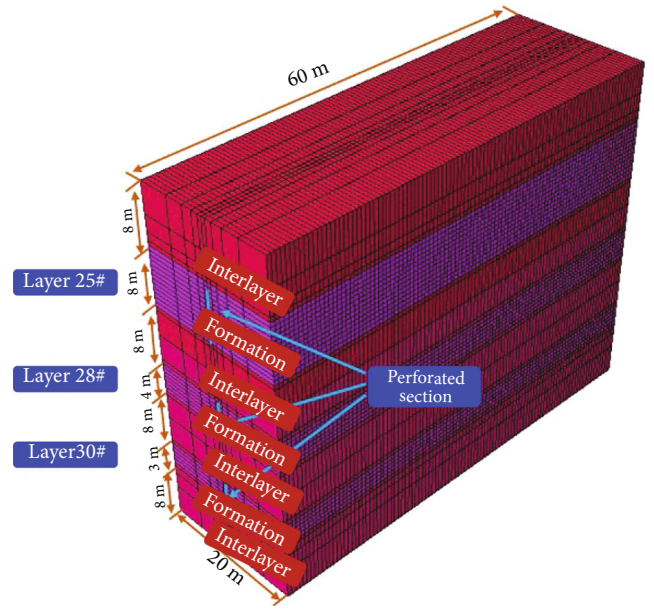

Figure 1: Model diagram of hydraulic fracturing perforated reservoir.

3. Optimization of Packing Parameters for Efficient Fracturing of Loose Sandstone

3.1. Mathematical Model. Sand-carrying fluid containing proppant enters the fracture, and the proppant will be moved to the front and bottom under the action of liquid resistance, its own gravity and liquid buoyancy. Delivery equation:

$$\frac{\partial}{\partial x}\left(C \cdot W \cdot u_{px}\right) + \frac{\partial}{\partial y}\left(C \cdot W \cdot u_{py}\right) + \frac{\partial}{\partial t}\left(C \cdot W\right) = 0. \quad (6)$$

Pressure drop equation:

$$\frac{dp(x,t)}{dx} = -\frac{64}{\pi}\frac{q(x)\mu}{h \cdot W^3}, \quad (7)$$

where C is the proppant concentration (sand ratio); W is the fracture width; u_{px} is the horizontal flow rate of the proppant; u_{py} is the settling velocity of the proppant; h is the fracture height; μ is the visible viscosity; p is the pressure inside the fracture.

It can be seen that the factors affecting the migration law of proppant mainly include filling parameters such as the viscosity of the sand-carrying liquid and the sand ratio. In this paper, the fracture propagation results of layer no. 30 in the abovementioned layered fracturing are used as the physical model, and the Euler-Eulerian model is used to further explore the effect of sand-carrying fluid viscosity and sand ratio on proppant migration in unconsolidated sandstone fractures through numerical simulation.

3.2. Influence of Sand-Carrying Fluid Viscosity. In order to explore the effect of sand-carrying fluid viscosity on proppant migration in fracturing fractures, the sand ratio was kept constant at 5%, and the sand-carrying fluid viscosity

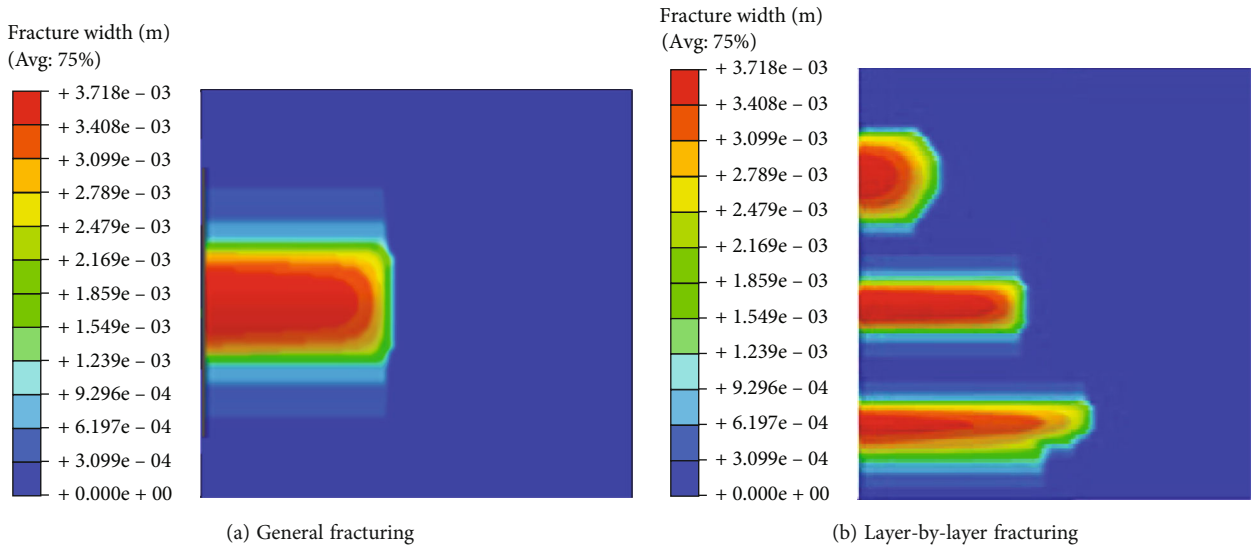

(a) General fracturing (b) Layer-by-layer fracturing

Figure 2: Sectional diagram of general fracturing and layered fracturing.

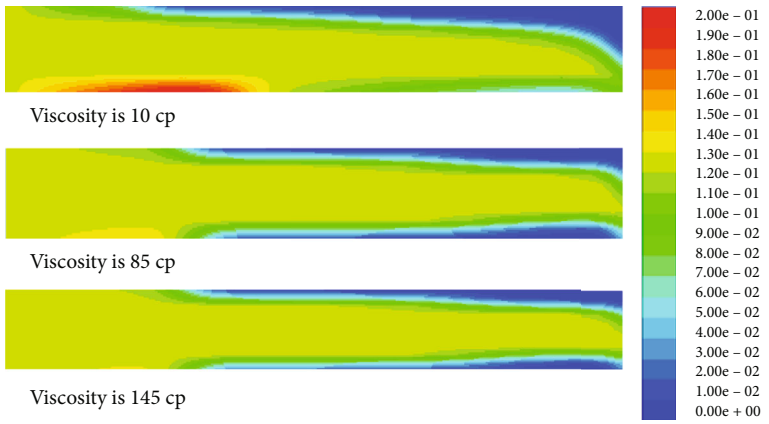

Figure 3: Proppant concentration diagram under different viscosities.

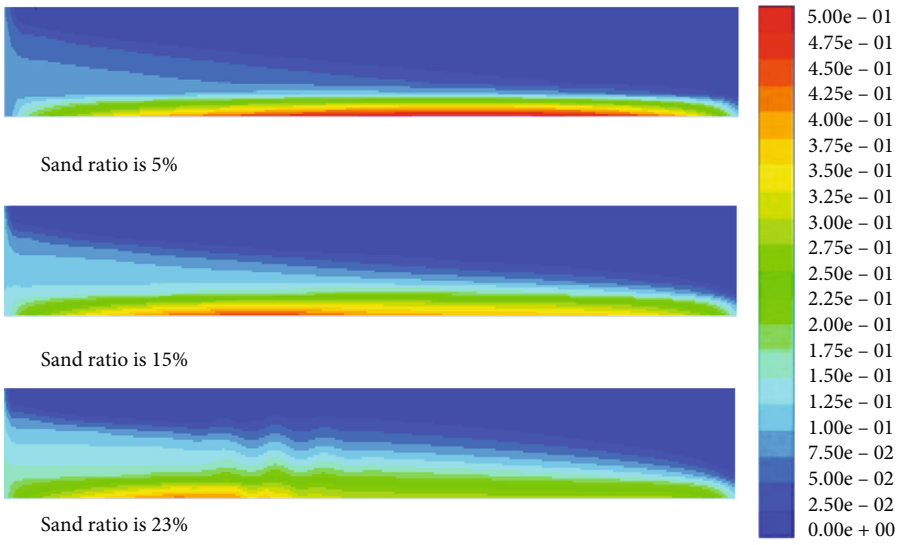

Figure 4: Proppant concentration map under different sand ratios.

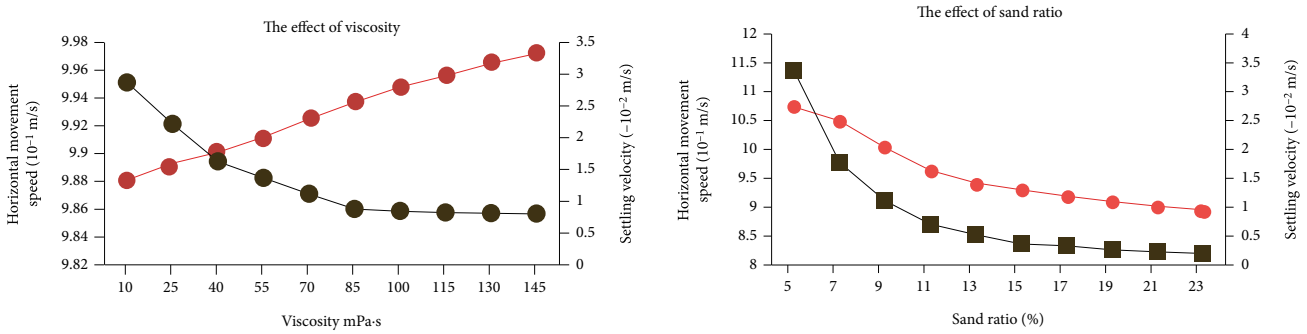

Figure 5: Variation rule of settling (black line) and horizontal velocity (red line) of proppant under different viscosity and sand ratio.

was set to 10–145 cp, every 15% cp is a gradient. The simulation results are analyzed, as shown in Figure 3. It can be seen from the figure that as the viscosity of the sand-carrying fluid increases, the proppant migration distance becomes longer; the darker the color, the greater the proppant concentration here. When the viscosity is 10 mPa•s, a large amount of proppant has begun to settle at the fracture entrance. When the viscosity of the sand-carrying fluid reaches 145 mPa•s, only a small amount of proppant settles at the fracture entrance, and most of the proppant is suspended in the center of the fracture.

3.3. Influence of Sand Ratio. In order to explore the effect of sand ratio on proppant migration in fracturing fractures, the viscosity of the sand-carrying fluid was kept constant at 85 cp, the sand ratio was set at 5% to 23%, and every 2% was a gradient. The simulation results of 5%, 15%, and 23% are selected for analysis, as shown in Figure 4. It can be seen from the figure that when the sand ratio increases, the proppant concentration at the bottom of the fracture decreases. When the sand ratio was 5%, the proppant concentration at the bottom of the fracture was higher, and when the sand ratio was 23%, the proppant concentration at the bottom was lower. It can be concluded that as the sand ratio increases, the settling velocity of the proppant decreases.

3.4. Filling Parameter Optimization. Carrying liquid and the sand ratio on the horizontal migration velocity and settling velocity of the proppant was further explored, as shown in Figure 5. It can be seen from the figure that increasing the viscosity of the sand-carrying liquid can reduce the settling velocity and, at the same time, increase the horizontal velocity, which is conducive to the migration of the proppant to the far end, but when the viscosity reaches 85 mPa•s, the change of the settling velocity is not obvious. The horizontal migration speed and settling speed of proppant will decrease with the increase of sand ratio, making it easy to suspend in fractures, but not easy to migrate to the far end. It can be seen from the simulation that the settling velocity of proppant can be reduced by changing the viscosity of the sand-carrying liquid. After the viscosity increases to a certain value, the sand ratio can be increased to continue to reduce the settling velocity of the proppant. However, the adjustment should be carried out within a small range to ensure that the proppant has sufficient horizontal velocity to migrate deep into the fracture. Therefore, parameters are optimized by increasing the viscosity and increasing the sand ratio in a small range.

Table 3: Optimization conditions of different filling parameters.

Numbering	Sand-carrying fluid viscosity (cp)	Sand ratio
1	10	5%
2	25	7%
3	40	9%
4	55	11%
5	70	13%
6	85	15%
7	100	17%
8	115	19%
9	130	21%
10	1 45	23%

Based on the above understanding, 10 groups of parameter optimization conditions are set, as shown in Table 3. The simulation results show that the horizontal migration velocity and settling velocity of proppant under different conditions change as shown in Figure 6. With the increase of sand-carrying fluid viscosity and sand ratio, the horizontal migration velocity of proppant decreased slightly but did not change much. Before the 6 sets of working conditions, the settling velocity decreased rapidly and then the decrease range was basically zero. Therefore, group 6 (liquid viscosity 85 mPa•s + sand ratio 15%) can be regarded as an ideal filling method.

4. Field Application

The study area is located at the southern end of the updip part of the western slope of the Liaohe fault depression in the Liaohe Oilfield. The oilfield structure is a nose-shaped structure cut by a fault. The reservoir type is a layered sandstone edge-bottom water reservoir, and the reservoir is shallow (1080~1950 m), with an average porosity and permeability of 26% and 0.98μm^2, respectively, which belongs to a typical high-porosity and high- permeability unconsolidated sandstone reservoir.

The fracturing and filling technology is the main means of stimulation and sand control in this block, but there is a

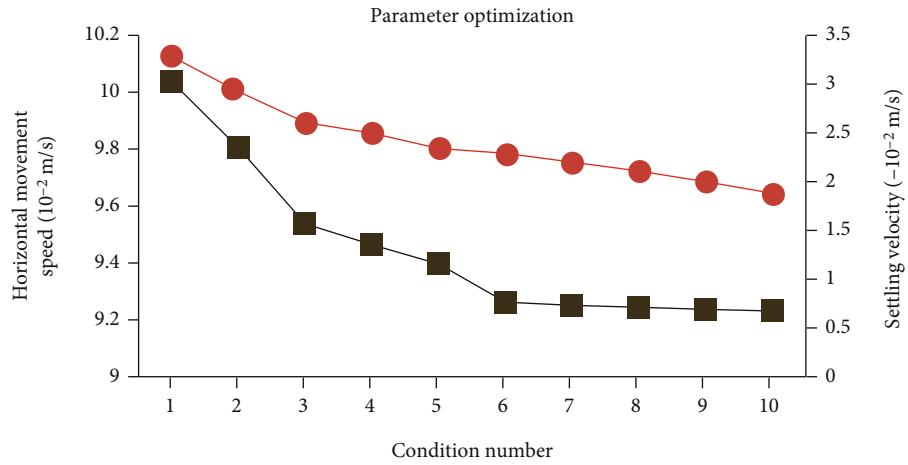

(a) Water migration (red line) and settling (black) velocity

(b) Preferred Results

Figure 6: Fill parameter optimization results.

Table 4: Design of construction parameters for efficient fracturing and filling.

Hashtag	Proppant particle size/mesh	Injection displacement/ (m^3/min)	Sand-carrying fluid viscosity/(mPa s)	Sand ratio/%	Total injection time/min
H27-1	20/40	2.3	9 0	1 5	4 0
H27-2	20/40	2.4	8 5	1 5	5 0
H27-3	20/40	2.3	9 0	1 5	4 5

Table 5: Comparison of the production conditions of the three wells and adjacent wells.

Hashtag	Initial production status			Current production		
	Liquid yield/ (m^3/d)	Oil production/ (m^3/d)	Production differential pressure/MP a	Liquid yield (m^3/d)	Oil production/ (m^3/d)	Production differential pressure/MP a _
H27-1	65~108	4 5 ~ 79	2.5 ~ 2.8 _	1 20~180	28~38	6.5 ~ 8.8 _
H27-2	4 8 ~ 96	3 4 ~ 68	2 .7 ~ 3.2	9 5 ~ 168	21~34	6.0 ~ 7.5 _
H27-3	3 7 ~ 75	2 5 ~ 59	2 .4 ~ 3.0	73~126	15~32	7.2 ~ 9.3 _
H 26-6	3 0 ~ 56	1 2 ~ 21	3.5 ~ 4.8 _	9 5 ~ 142	6 ~ 11	9.8 ~ 12.3 _

lack of reasonable optimization methods for filling parameters in the early stage, and the parameter setting relies on the reference of adjacent wells and empirical judgment, resulting in unstable production, easy sand production, and rapid decay of each production well. And other problems occur frequently. Combined with the optimization technology of high-efficiency fracturing and filling parameters of loose sandstone proposed in this study, combined with the production data of adjacent wells and the results of lithology analysis, the three wells are H 27-1, H 27-2, and H 27-3. The filling parameters were optimized, and the specific construction parameters of each well are shown in Table 4.

The production results of the three wells and the historical production data of the adjacent wells are shown in Table 5. The analysis shows that the stable production pressure difference of the three wells is maintained between 6 and 9.3 MPa, and the daily oil production at the initial stage of production and after stable production is higher than that of the adjacent well H. Well 26-6, the increase was 2.5 to 3.4 times. The results of this work are heavily dependent on numerical simulation, and applicability of the proposed optimization method on realistic oil wells requires further clarification.

5. Conclusions

(1) In unconsolidated sandstone formations, the cross-sectional area of fractures formed by layered fracturing is much larger than that of general fracturing, and layered fracturing should be selected. The mechanism of fracture initiation and extension is closely related to the formation permeability, and the higher the permeability, the smaller the fracture length, the larger the fracture width and fracture height

(2) Increasing the viscosity of the sand-carrying liquid can significantly reduce the settling velocity and increase the horizontal velocity, which is conducive to the migration of the proppant to far end. The horizontal velocity and settling velocity of the proppant will decrease with the increase of the sand ratio, making it easier to suspend in the fracture, but not conducive to distal migration. The optimal filling parameters are 85 mPa•s and 15% of the sand-carrying liquid viscosity

(3) Field application results show that the daily oil production of the three production wells after using the loose sandstone high-efficiency filling parameter optimization technology is higher than that of the adjacent wells at the initial stage of production and after stable production, which is increased by 2.5-3.4 times

Data Availability

Data available on request.

Ethical Approval

On behalf of all the coauthors, the corresponding author states that there are no ethical statements contained in the manuscripts.

Conflicts of Interest

The author declares that there is no conflicts of interest regarding the publication of this paper.

References

[1] X. Guomin and G. Zhongmin, "Research and test of chemical flooding technology in unconsolidated sandstone reservoirs [J]," *Special Oil and Gas Reservoirs*, vol. 27, no. 6, pp. 139–144, 2020.

[2] Z. Xiaocheng, W. Xiaopeng, L. Jin, H. Yaotu, and Z. Ming, "Research and application of fracturing and packing technology of loose sandstone in Bohai oilfield[J]," *Petroleum Machinery*, vol. 49, no. 9, pp. 66–72, 2021.

[3] D. Ma, H. Duan, J. Zhang, X. Liu, and Z. Li, "Numerical simulation of water-silt inrush hazard of fault rock: a three-phase flow model," *Rock Mechanics and Rock Engineering*, vol. 55, no. 8, pp. 5163–5182, 2022.

[4] D. Ma, H. Duan, and J. Zhang, "Solid grain migration on hydraulic properties of fault rocks in underground mining tunnel: radial seepage experiments and verification of permeability prediction," *Tunnelling and Underground Space Technology*, vol. 126, article 104525, 2022.

[5] L. Yechun, "Characteristics of digital core seepage in high argillaceous loose sandstone reservoirs in Western South China Sea oilfield[J]," *China Offshore Oil & Gas*, vol. 27, no. 4, pp. 86–92, 2015.

[6] D. Jingen, W. Jinfeng, and Y. Jianhua, "Study on the propagation law of hydraulic fracturing fractures in weakly consolidated sandstone gas reservoirs[J]," *Rock and Soil Mechanics*, vol. 1, pp. 72–74, 2002.

[7] K. Agarwal and M. M. Sharma, "A new approach to modeling fracture growth in unconsolidated sands," in *SPE Annual Technical Conference and Exhibition, Society of Petroleum Engineers*, Colorado, 2011.

[8] Z. Shaowei, M. Yingwen, L. Feihang, L. Haitao, and Z. Jianfeng, "Fracture model of loose sandstone based on linear strengthening [J]," *Chinese Journal of Petroleum*, vol. 40, no. S2, pp. 131–140, 2019.

[9] L. Hai, D. Jingen, L. Wei, X. Xie Tao, and L. H.-l. Jie, "Numerical simulation of hydraulic fracture propagation in weakly consolidated sandstone reservoirs," *Journal of Central South University*, vol. 25, no. 12, pp. 2944–2952, 2018.

[10] Z. Peiyu, L. Jianwei, L. Tianjun, L. Luo, and Z. Yanwen, "Research and application of fracturing and sand control technology in Yanmuxi loose sandstone reservoir[J]," *Drilling and Production Technology*, vol. 37, no. 6, pp. 49–51, 2014.

[11] F. Baitao, D. Jingen, W. Lin Hai, L. W. Rui, and T. Qiang, "Numerical simulation of fracture propagation law in unconsolidated sandstone reservoirs[J]," *Petroleum Drilling and Production Technology*, vol. 40, no. 5, pp. 626–632, 2018.

[12] L. Mingzhong, X. Jiaqi, and Q. Minhui, "Simulation study of sanding region prediction in unconsolidated reservoir with frac-pack[J]," *IOP Conference Series: Earth and Environmental Science*, vol. 632, no. 2, article 022001, 2021.

[13] Z. Sun, S. Wang, H. Xiong, K. Wu, and J. Shi, "Optimal nanocone geometry for water flow," *AICHE Journal*, vol. 68, no. 3, article e17543, 2022.

[14] Z. Sun, B. Huang, Y. Liu et al., "Gas-phase production equation for CBM reservoirs: interaction between hydraulic fracturing and coal orthotropic feature," *Journal of Petroleum Science and Engineering*, vol. 213, article 110428, 2022.

[15] W. U. Rui, *Study on Deformation and Failure Mechanism of Weakly Cemented Unconsolidated Sandstone Reservoirs[D]*, China University of Petroleum(Beijing), 2018.

[16] L. Yong, C. Yao, J. Jianzhou, J. Le, D. Feng, and Y. Xiong, "Cement hull interface fracture propagation under volume fracturing in shale gas wells[J]," *Journal of Petroleum*, vol. 38, no. 1, pp. 105–111, 2017.

[17] S. Keming, Z. Shucui, and L. Tianshu, "Study on the propagation law of hydraulic fracturing cracks in transversely isotropic oil and gas reservoirs[J]," *Journal of Computational Mechanics*, vol. 33, no. 5, pp. 767–772, 2016.